Journal of King Saud University – Science 31 (2019) 1014–1019

Contents lists available at ScienceDirect

Journal of King Saud University – Science

journal homepage: www.sciencedirect.com

Local discontinuous Galerkin method for the nonlocal one-way water wave equation

Shuming Liu, Can Li *

Department of Applied Mathematics, School of Sciences, Xi'an University of Technology, Xi'an, Shaanxi 710054, People's Republic of China

ARTICLE INFO

Article history:
Received 1 July 2018
Accepted 7 November 2018
Available online 10 November 2018

Keywords:
Nonlocal water wave equation
Local discontinuous Galerkin method

ABSTRACT

In this paper, we develop a local discontinuous Galerkin (LDG) method for numerically solving the nonlocal one-way water wave equation. Based on the features of fractional derivative, the considered model is first coupled into a classical first derivative and a nonlocal fractional integral. Then LDG algorithm is used in space discretization by properly choosing the numerical fluxes. Numerical examples are provided to show the accuracy and effectiveness.

1. Introduction

The study of water waves governed by Euler equations has interested researchers over many years. Under appropriate assumption, the irrotational Euler equations with zero surface tension reduces to the following water wave equation (Wu, 1997; Jennings, 2012; Beale et al., 1993)

$$u_{tt} + \partial_x \mathcal{H} u(x,t) = F(u,t), \quad x \in R, \ t > 0, \tag{1.1}$$

where $\mathcal{H}$ denotes the Hilbert transform

$$\mathcal{H}(u)(x) = \frac{1}{\pi}\, p.v. \int_{-\infty}^{+\infty} \frac{u(y)}{x-y} dy, \tag{1.2}$$

and the nonlinear term F consisting of the nonlinear terms. The linearized form of model (1.1) gives

$$u_{tt} + \partial_x \mathcal{H} u(x,t) = 0, \quad x \in R, \ t > 0. \tag{1.3}$$

In frequency space, nonlocal model (1.3) has the dispersion relation $(2\pi w)^2 = |2\pi k|$, which means

$$w = \pm \mathrm{sgn}(k)\sqrt{\frac{|k|}{2\pi}}. \tag{1.4}$$

Applying the inverse the Laplace-Fourier transform, in physical space, Eq. (1.4) becomes two one-way water wave equations

$$u_t \pm \frac{1}{\sqrt{2\pi}} \partial_x \left(\int_{-\infty}^{+\infty} \frac{u(y,t)}{\sqrt{|x-y|}} dy \right) = 0, \tag{1.5}$$

where the $(+)$ corresponds to right-going waves and the $(-)$ to left-going waves. Recalling the left Riemann-Liouville integral (Podlubny, 1999)

$${}_{-\infty}D_x^{-1/2} u(x,t) = \frac{1}{\sqrt{\pi}} \int_{-\infty}^{x} \frac{u(y,t)}{\sqrt{x-y}} dy,$$

and the right Riemann-Liouville integral (Podlubny, 1999)

$${}_xD_{+\infty}^{-1/2} u(x,t) = \frac{1}{\sqrt{\pi}} \int_{x}^{+\infty} \frac{u(y,t)}{\sqrt{y-x}} dy,$$

the nonlocal model (1.5) can be expressed as

$$u_t(x,t) \pm \frac{1}{\sqrt{2}} \partial_x \left({}_{-\infty}D_x^{-1/2} + {}_xD_{+\infty}^{-1/2} \right) u(x,t) = 0. \tag{1.6}$$

Numerical studies of nonlocal water waves equation have been performed in recent works (Chen et al., 2012; Jennings, 2012; Jennings et al., 2014; Li and Zhao, 2016). The LDG method has been intensively studied and successfully applied to solve various linear and nonlinear partial differential equations since it was first introduced by Cockburn and Shu (1998). We refer to Hesthaven and Warburton, 2008, Shu (2016) and references cited therein for the development of LDG methods. Recently, there has been a growing interest in LDG methods for space fractional diffusion problems (Ji and Tang, 2012; Deng and Hesthaven, 2013; Xu and Hesthaven, 2014; Mao and Kamiadakis, 2017). The numerical test results show that the LDG method provides a very effective numerical method

* Corresponding author.
E-mail address: mathlican@xaut.edu.cn (C. Li).

Peer review under responsibility of King Saud University.

Production and hosting by Elsevier

https://doi.org/10.1016/j.jksus.2018.11.003
1018-3647/

for solving nonlocal fractional diffusion equations. Recently, in view of conservative form (1.5), Jennings et al. present a semi-discrete finite volume scheme for (1.5) by using piecewise polynomial reconstruction. Motivated by the work (Ji and Tang, 2012), we will design a highly accurate local discontinuous Galerkin method for the nonlocal conservative form (1.5). The LDG method is constructed by using choosing numerical flux instead of using polynomial reconstruction.

The content of the paper is organized as follows. In Section 2, we present the formulation of the semi-discrete LDG methods for model (1.5). To verify the effectiveness of the proposed LDG scheme, the extensive numerical results are presented in Section 3. Concluding remarks is summarized in Section 4.

2. Formulation of local discontinuous Galerkin method

We design the LDG method for model (1.6) in finite domain $[a,b]$, and we always assume that the solution of model (1.6) has support on $[a,b]$. To design the LDG method for model (1.6), we introduce auxiliary variable $v(x,t)$, then the model (1.6) can be rewritten as

$$\begin{cases} u_t(x,t) - \partial_x v(x,t) = 0, \\ v(x,t) \pm \frac{1}{\sqrt{2}}\left({}_aD_x^{-1/2} + {}_xD_b^{-1/2}\right)u(x,t) = 0. \end{cases}$$

Let $a = x_{\frac{1}{2}} < x_{\frac{3}{2}} < \cdots < x_{N+\frac{1}{2}} = b$ be any regular partition of $[a,b]$ with mesh step $h_j = x_{j+\frac{1}{2}} - x_{j-\frac{1}{2}}$ and $h = \max_{1\leqslant j\leqslant N} h_j$. Denote $x_{j+\frac{1}{2}} = \frac{1}{2}(x_j + x_{j+1})$ and $I_j = [x_{j-\frac{1}{2}}, x_{j+\frac{1}{2}}]$. The piecewise polynomials of degree at most k over the subintervals V_h on the cell I_j is defined as $V_h = \{v : v \in P^k(I_j), x \in I_j\}$. The semi-discrete LDG scheme is defined as follows. Find $u_h(\cdot,t) \in V_h$ and $v_h(\cdot,t) \in V_h$, such that for any $\phi \in V_h$ and $\psi \in V_h$,

$$\begin{cases} (u_{ht}, \phi)_{I_j} + (v_h, \phi_x)_{I_j} - \hat{v}_h \phi|_{x^+_{j-\frac{1}{2}}}^{x^-_{j+\frac{1}{2}}} = 0, \\ (v_h, \psi(x))_{I_j} \pm \frac{1}{\sqrt{2}}\left({}_aD_x^{-1/2}u + {}_xD_b^{-1/2}u, \psi(x)\right)_{I_j} = 0, \\ (u_h(x,0), \phi(x))_{I_j} = (u_0(x), \phi(x))_{I_j}, \end{cases} \tag{2.1}$$

where $\hat{v}_h$ denotes the numerical flux. We use the alternating direction flux (Cockburn and Shu, 1998), defined as

$$\hat{u}_{j+\frac{1}{2}} = u^-_{j+\frac{1}{2}}, \quad \hat{v}_{j+\frac{1}{2}} = v^+_{j+\frac{1}{2}}, \quad 0 \leqslant j \leqslant N-1.$$

or

$$\hat{u}_j = u^+_{j+\frac{1}{2}}, \quad \hat{v}_{j+\frac{1}{2}} = v^+_{j+\frac{1}{2}}, \quad 0 \leqslant j \leqslant N-1.$$

where $u^\pm(x_j) = \lim_{x\to x_j^\pm} u(x)$, $[u] = u^+ - u^-$. For the numerical flux at the boundary, we use the flux introduced in Castillo et al. (2003), in the form

$$\hat{u}_{N+\frac{1}{2}} = u(b,t), \quad \hat{v}_{N+\frac{1}{2}} = v^-_{N+\frac{1}{2}} + \frac{\gamma}{h}[u_{N+\frac{1}{2}}].$$

or

$$\hat{u}_{\frac{1}{2}} = u(a,t), \quad \hat{v}_{\frac{1}{2}} = v^-_{\frac{1}{2}} + \frac{\gamma}{h}[u_{\frac{1}{2}}],$$

where γ is a positive constant. Let $\{t_n\}_{n=0}^{N_t}$ be a partition of time interval $[0,T]$ with the time step size Δt. Denote vector $\mathbf{u}_h$ be the unknown coefficients of numerical solutions, then the discrete ODE system (2.1) can be written as

$$\frac{d\mathbf{u}_h}{dt} = \mathcal{L}(\mathbf{u}_h, t), \tag{2.2}$$

where $\mathcal{L}$ is produced by (2.1). For the time discretization of system (2.2), we use the third order explicit total variation diminishing (TVD) Runge-Kutta method (Gottlieb et al., 2001)

$$\begin{aligned} \mathbf{u}_h^{(1)} &= \mathbf{u}_h^n + \Delta t \mathcal{L}(\mathbf{u}_h^n, t_n), \\ \mathbf{u}_h^{(2)} &= \frac{4}{3}\mathbf{u}_h^n + \frac{1}{4}\mathbf{u}_h^{(1)} + \frac{1}{4}\Delta t \mathcal{L}\left(\mathbf{u}_h^{(1)}, t^n + \Delta t\right), \\ \mathbf{u}_h^{n+1} &= \frac{1}{3}\mathbf{u}_h^n + \frac{2}{3}\mathbf{u}_h^{(2)} + \frac{2}{3}\Delta t \mathcal{L}\left(\mathbf{u}_h^{(2)}, t_n + \frac{1}{2}\Delta t\right). \end{aligned} \tag{2.3}$$

3. Numerical results

In this section, we present two numerical examples to show the accuracy and the performance of the method for the considered model. In our examples, the condition $\Delta t \leqslant Ch^{(k+1)/3}$ $(0 < C < 1)$ is used to fulfill the stability. In the first example, we examine the accuracy with piecewise P^k polynomial approximations. The errors are measured by L^2 and L^∞ norms. The computed convergence order are calculated by

$$\text{order} = \frac{\log(E(h)) - \log(E(h/2))}{\log(2)},$$

where $E(h)$ is the L^2 or L^∞-error calculated in the spatial step h. The second example, we simulate the propagation of left and right one-way water wave equations with a special wave packet.

Example 1. Consider the one-way left-going water wave Eq. (1.6) on the finite domain $x \in (0,1)$, $t \in [0,1]$. We chose $u(x,t) = e^{-t}x^6(1-x)^6$ as the exact solution of problem (1.6), and add a source term $f(x,t)$ on the right side of (1.6). The initial-boundary conditions are determined by the exact solution.

Tables 1–2 report the numerical errors and convergence orders for the discrete solutions computed by numerical scheme (2.1). We observe that the accuracy of the LDG scheme are of order $k+1/2$ for $k = 1,2$, is of order $k+1$ for $k = 3$ in both L^2 and L^∞ norms. In the numerical flux at the boundary, we take $\gamma = 0.05$ in our computation. To test the stability of the numerical scheme, we rewrite the discrete ODE system (2.2) as

$$\frac{d\mathbf{u}_h(t)}{dt} = A\mathbf{u}_h(t), \tag{3.1}$$

where the iterate matrix A is dense due to the nonlocal term of scheme (2.1). Let $\{\lambda_k\}$ be the eigenvalues of matrix A. We compute their by numerical method because the analytically form can't obtain. To check the numerical stability of TVD Runge-Kutta method, we denote $g(z)$ be the amplification factor of the scheme (2.3). If the numerical scheme (2.3) is stable, we require

$$\max_k |g(\nu\lambda_k)| \leqslant 1, \tag{3.2}$$

where $\nu = \frac{h}{\sqrt{\Delta t}}$. The Eigenvalues of A for $k = 1$, $k = 2$, and $k = 3$ are plotted in Fig. 1. The distribution of $\max_k |g(\nu\lambda_k)|$ for $k = 1$, $k = 2$ and $k = 3$ are given in Figs. 2, 3 and 4, respectively.

Example 2. Consider the problem (1.6) with the wave packet (Jennings, 2012; Jennings et al., 2014)

$$u(x,0) = \begin{cases} \cos^6\left[\frac{\pi}{6}20(x-\frac{1}{2})\right]\sin\left[\frac{5\pi}{6}20(x-\frac{1}{2})\right], & 0.35 < x < 0.65, \\ 0, & \textit{otherwise}. \end{cases} \tag{3.3}$$

Table 1
The L^2 errors and convergence orders of u computed by the numerical scheme (2.1) for Example 1.

h	P^1		P^2		P^3	
	L^2 error	order	L^2 error	order	L^2 error	order
1/5	1.1881e−05		2.4200e−06		2.0483e−06	
1/10	3.9638e−06	1.5837	4.0077e−07	2.5942	1.0216e−07	3.8646
1/20	1.3638e−06	1.5393	6.4181e−08	2.6426	5.7122e−09	4.3255
1/40	4.6965e−07	1.5380	1.0403e−08	2.6251	4.4589e−10	3.6793

Table 2
The L^∞ errors and convergence orders of u computed by the numerical scheme (2.1) for Example 1.

h	P^1		P^2		P^3	
	L^∞ error	order	L^∞ error	order	L^∞ error	order
1/5	3.7583e−05		7.3163e−06		5.0434e−06	
1/10	1.4405e−05	1.3835	1.4028e−06	2.3828	3.7335e−07	3.7558
1/20	5.2161e−06	1.4655	2.3655e−07	2.5681	1.9811e−08	4.2362
1/40	1.7632e−06	1.5648	3.5806e−08	2.7239	1.3744e−09	3.8494

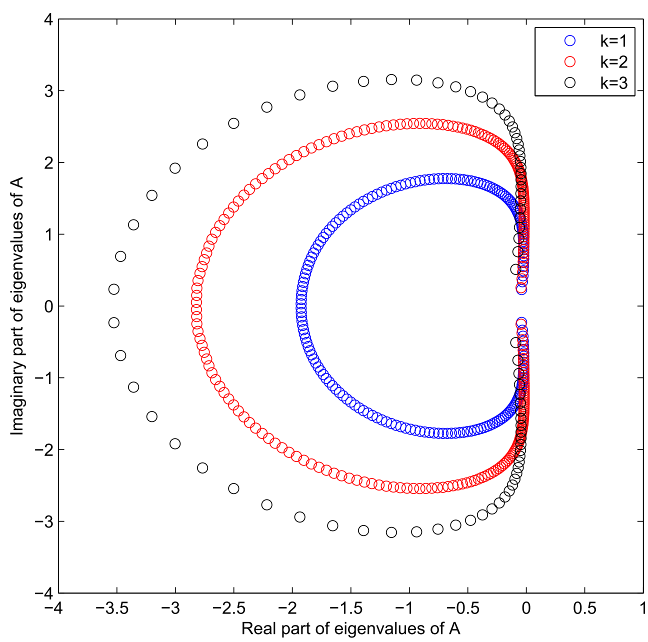

Fig. 1. Eigenvalues of A for $k = 1$, $k = 2$, and $k = 3$.

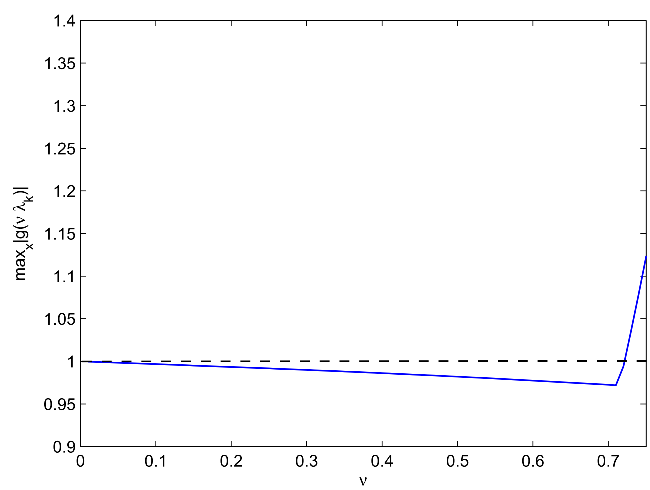

Fig. 3. The distribution of $\max_k|g(\nu\lambda_k)|$ for $k = 2$.

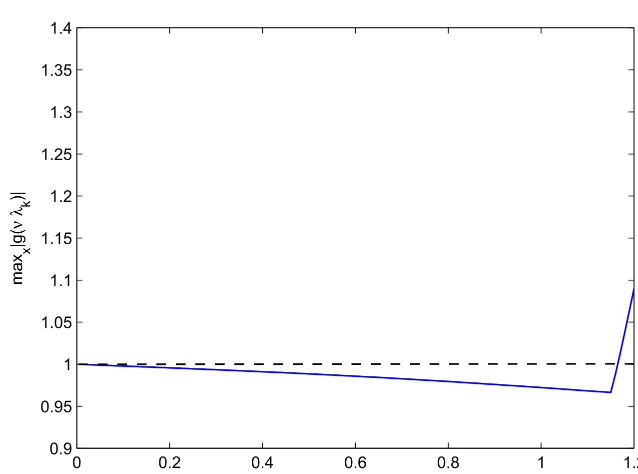

Fig. 2. The distribution of $\max_k|g(\nu\lambda_k)|$ for $k = 1$.

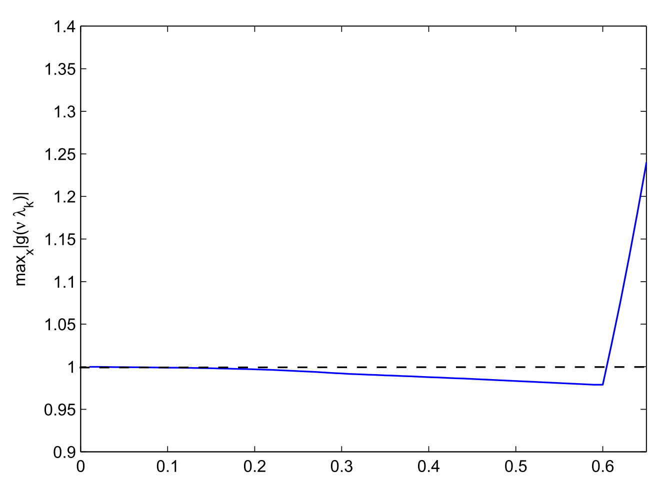

Fig. 4. The distribution of $\max_k|g(\nu\lambda_k)|$ for $k = 3$.

Table 3
The L^2 errors and convergence orders of left going wave u computed by the LDG method for Example 2.

h	P^1 L^2 error	P^1 order	P^2 L^2 error	P^2 order
1/40	8.9960e−02		1.1279e−01	
1/80	4.1771e−02	1.1068	4.0618e−02	1.4734
1/160	1.4719e−02	1.5048	6.5961e−03	2.6624

The exact solution of (1.6) in not available. To test the effective rate of convergence, we chose u_{exact} as the "exact" solution which is computed at a fine grid $h = 1/200$. The errors and orders of accuracy for numerical solutions are reported in Table 3. We observe that the method with P^k elements gives a uniform almost $(k+1)$th order of accuracy for LDG solutions in L^2 norm.

We test the wave propagation of the problem (1.6) with wave packet (3.3). The simulation of wave propagation for left and right -going waves are listed in Figs. 5–8. We take $[0, 1]$ as the computational domain and use the P^2 element with $N = 40$ in our computation. We can see that the moving wave profile is resolved very well. From Figs. 7–8, we can see that the same results can be obtained by using less mesh girds points compared with the method given in Jennings et al. (2014).

Finally, we discuss the long time behavior of solutions to the one way water wave (1.6) using the LDG method (2.1). It is proved that the solutions of (1.6) decays at the rate $\max_x|u(x,t)| = O(t^{-1/2}),\ t \to \infty$. We compute the solution on the domain $(0, 1)$ until time $t = 6$. For $n = 1$ to 100, we compute $\max_x|u(x,t)|$. Fig. 9 shows n plotted versus $\max_x|u(x,t)|$. From Fig. 9, we can see the numerical solution decays at the rate $O(t^{-1/2})$, which confirms the theoretical results given by Jennings et al. (2014).

4. Conclusion

Inspired by the nature of fractional derivative, we present a local DG methods for the nonlocal one-way water wave equation. The main idea of our method are that the fractional derivative is splitted into a classical first derivative and a nonlocal fractional integral, then the semi-discrete LDG method is designed by carefully choosing the numerical flux. The semi-discrete system is computed by the third order TVD Runge-Kutta method. The numerical scheme is verified for the smooth solution, and some numerical solutions is simulated. Numerical results show that the method with P^k elements don't give an optimal $k+1$ order of accuracy. We will carry out the details of error estimates in our next work. Finally, numerical simulation shows that our LDG method works well for the one-way water wave equation.

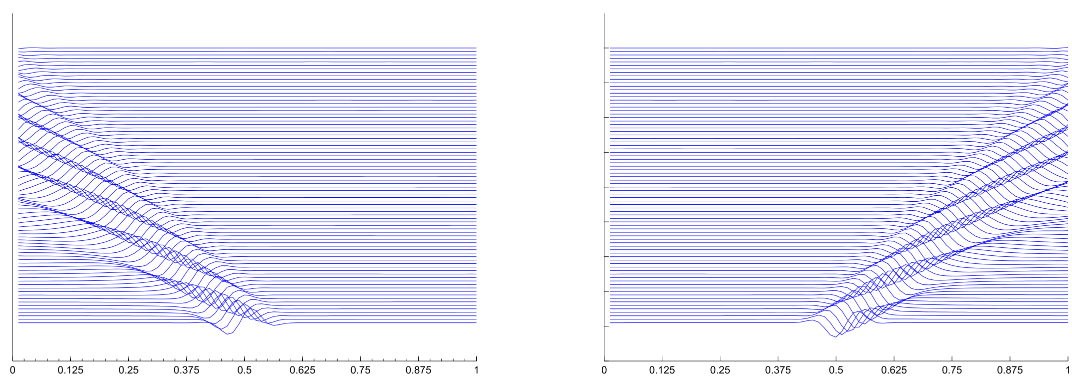

(a) Left one-way water wave. (b) Right one-way water wave.

Fig. 5. The evolution of left (a) and right (b) going one-way water wave equations with wave packet (3.3).

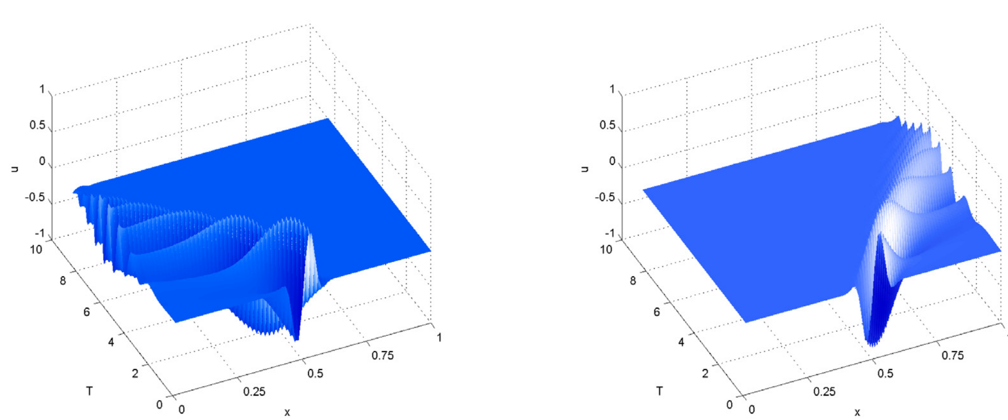

(a) Left one-way water wave. (b) Right one-way water wave.

Fig. 6. The evolution of left (a) and right (b) going one-way water wave equations with wave packet (3.3).

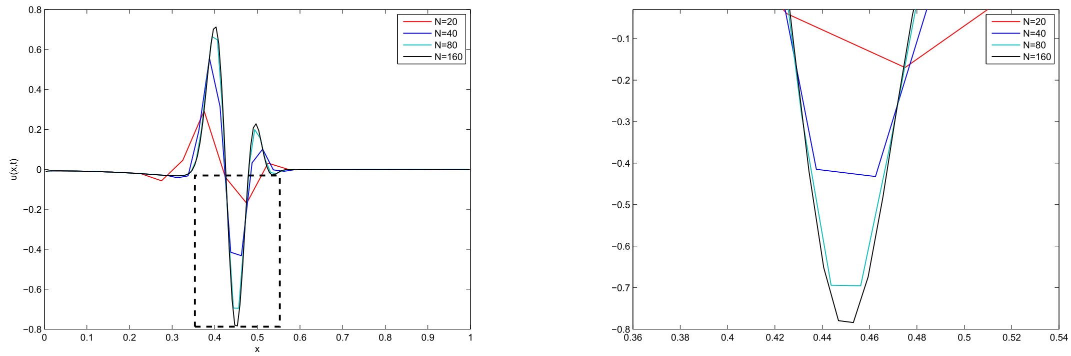

(a) Left one-way water wave. (b) Boxed region.

Fig. 7. Wave profile for left one-way water waves (a) and boxed region (b) computed by piece wise linear polynomial with wave packet (3.3).

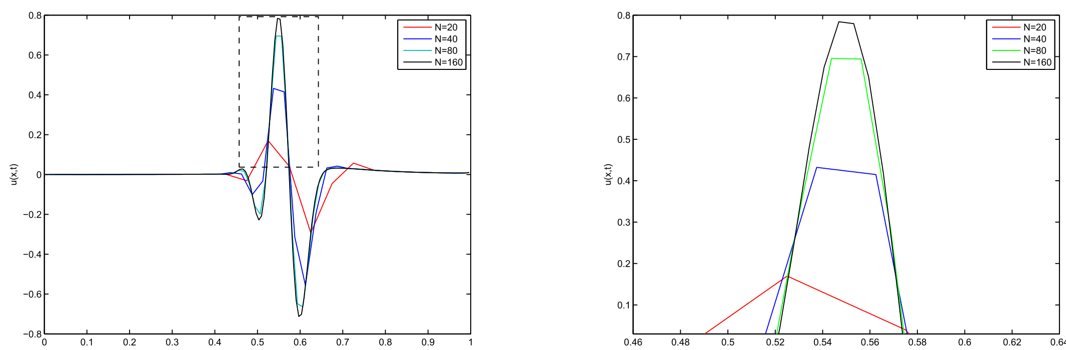

(a) Right one-way water wave. (b) Boxed region.

Fig. 8. Wave profile for right one-way water waves (a) and boxed region(b) computed by piece wise linear polynomial with wave packet (3.3).

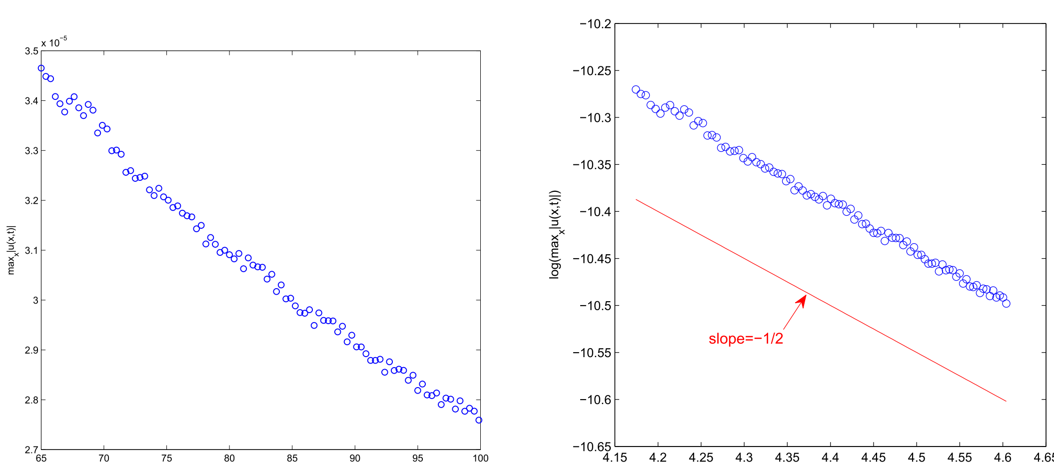

(a) The decay rate of left-going one-way WWE. (b) Boxed region.

Fig. 9. The decay rate of left-going one-way water waves (a) and boxed region (b) computed with initial data (3.3).

Conflicts of interest

The authors declare that there is no conflict of interests regarding the publication of this paper.

Acknowledgments

We would like to thank the editor and anonymous referees for their many valuable comments and suggestions.

References

Beale, J., Hou, T., Lowengrub, J., 1993. Growth rates for the linearized motion of fluid interfaces away from equilibrium. Commun. Pure Appl. Math 46 (9), 1269–1301.
Castillo, P., Cockburn, B., Schötzau, D., Schwab, C., 2003. Optimal a priori error estimates for the hp-version of the local discontinuous galerkin method for convection-diffusion problems. Math. Comp 71 (238), 455–478.
Chen, M., Dumont, S., Goubet, O., 2012. Decay of solutions to a viscous asymptotical model for water waves: Kakutani-Matsuuchi model. Nonlinear Anal.: T.M.A 75 (5), 2883–2896.
Cockburn, B., Shu, C., 1998. The local discontinuous galerkin method for time-dependent convection-diffusion systems. SIAM J. Numer. Anal. 35 (6), 2440–2463.
Deng, W., Hesthaven, J., 2013. Local discontinuous galerkin methods for fractional diffusion equations. ESAIM Math. Model. Numer. Anal. 47 (6), 1845–1864.
Gottlieb, S., Shu, C., Tadmor, E., 2001. Strong stability-preserving high-order time discretization methods. SIAM Rev. 43 (1), 89–112.
Hesthaven, J., Warburton, T., 2008. Nodal Discontinuous Galerkin Methods. Algorithms, Analysis, and Applications. Springer, Berlin.
Jennings, G., 2012. Efficient Numerical Methods for Water Wave Propagation in Unbounded Domains Ph.D. Thesis. University of Michigan.
Jennings, G., Prigge, D., Carney, S., Karni, S., Rauch, J., Abgrall, R., 2014. Water wave propagation in unbounded domains. Part II: numerical methods for fractional pdes. J. Comput. Phys. 275 (1), 443–458.
Ji, X., Tang, H., 2012. High-order accurate Runge-Kutta (local) discontinuous galerkin methods for one-and two-dimensional fractional diffusion equations. Numer. Math. Theor. Methods Appl. 5 (3), 333–358.
Li, C., Zhao, S., 2016. Efficient numerical schemes for fractional water wave models. Comput. Math. Appl. 71 (1), 238–254.
Mao, Z., Kamiadakis, G., 2017. Fractional burgers equation with nonlinear non-locality: spectral vanishing viscosity and local discontinuous galerkin methods. J. Comput. Phys. 336 (1), 143–163.
Podlubny, I., 1999. Fractional differential equations. an introduction to fractional derivatives, fractional differential equations, some methods of their solution and some of their applications. New York.
Shu, C., 2016. High order weno and dg methods for time-dependent convection-dominated pdes: a brief survey of several recent developments. J. Comput. Phys. 316 (C), 598–613.
Wu, S., 1997. Almost global wellposedness of the 2-d full water wave problem. Invent. Math. 177 (1), 45–135.
Xu, Q., Hesthaven, J., 2014. Discontinuous Galerkin method for fractional convection-diffusion equations. SIAM J. Numer. Anal. 52 (1), 405–423.